*Proc. Natl. Acad. Sci. USA*
Vol. 92, pp. 2249–2253, March 1995
Developmental Biology

# Expression of the zinc-finger gene *PLZF* at rhombomere boundaries in the vertebrate hindbrain

(leukemia/segmentation/transcription factor/liver/translocation)

M. COOK*, A. GOULD*, N. BRAND†, J. DAVIES‡, P. STRUTT‡, R. SHAKNOVICH§, J. LICHT§, S. WAXMAN§, Z. CHEN¶, S. GLUECKSOHN-WAELSCH‖, R. KRUMLAUF*, AND A. ZELENT‡**

*Laboratory of Developmental Neurobiology, Medical Research Council National Institute for Medical Research, Mill Hill, London NW7 1AA, United Kingdom; †Department of Cardiothoracic Surgery, National Heart and Lung Institute, London SW3 6LY, United Kingdom; ‡Leukaemia Research Fund Centre at the Institute of Cancer Research, Chester Beatty Laboratories, Fulham Road, London SW3 6JB, United Kingdom; §Department of Medicine, Mount Sinai School of Medicine, New York, NY 10029; ¶Shanghai Institute of Haematology, Rui-Jin Hospital, Shanghai Second Medical University, Shanghai 200025, China; and ‖Department of Molecular Genetics, Albert Einstein College of Medicine, Bronx, NY 10461

*Contributed by Salome G. Waelsch, December 7, 1994*

**ABSTRACT** **To investigate the potential biological role(s) of the *PLZF* gene, discovered as a fusion with the *RARA* locus in a patient with acute promyelocytic leukemia harboring a t(11;17) chromosomal translocation, we have isolated its murine homologue (m*PLZF*) and studied its patterns of developmental expression. The levels of mPLZF mRNAs increased perinatally in the liver, heart, and kidney, but with the exception of the heart, they were either absent or very low in the adult tissues. *In situ* analysis of m*PLZF* expression in mouse embryos between 7.0 and 10.5 days of development revealed that mPLZF mRNAs and proteins were coexpressed in spatially restricted and temporally dynamic patterns in the central nervous system. In the hindbrain region, a segmental pattern of expression correlated with the development of the rhombomeres. From 9.0 days of development, starting first in rhombomeres 3 and 5, there was an ordered down-regulation of expression in the center of each rhombomere, so that 1 day later elevated levels of mPLZF mRNAs and proteins were restricted to cells surrounding the rhombomeric boundaries. The chicken homologue of the *PLZF* gene, which we have also cloned, demonstrated a similar segmental pattern of expression in the hindbrain. To date, *PLZF* represents the only example of a transcription factor with elevated expression at rhombomeric boundaries. The high degree of evolutionary conservation between the patterns of *PLZF* expression during mammalian and avian central nervous system development suggests that it has an important functional role in the regionalization of the vertebrate hindbrain, potentially regulating boundary cell interactions.**

Acute promyelocytic leukemia is generally associated with t(15;17) chromosomal translocation, which fuses the *RARA* locus with a gene called *PML* (1, 2). The importance of a retinoid signaling pathway(s) in the molecular pathogenesis of acute promyelocytic leukemia was underlined by the recent discovery of a patient with acute promyelocytic leukemia and a variant t(11;17) reciprocal chromosomal translocation that also involves the *RARA* gene (3). Molecular characterization of the t(11;17) led to the discovery of the human promyelocytic leukemia zinc finger gene (h*PLZF*) (3), a member of a gene family encoding transcription factors with characteristic $C_2$-$H_2$ zinc-finger (Zn-finger) DNA-binding motifs (4). Two different PLZF mRNA isoforms (A and B), which differ in one exon encoding proline-rich sequences, have been identified. In contrast to *PML*, initial studies have indicated that h*PLZF* is expressed in a tissue-specific manner and suggested a specific role for the hPLZF protein(s) in hemopoiesis (3); however, the function of *PLZF* during normal mammalian development remained unexplored.

Among the members belonging to the $C_2$-$H_2$ Zn-finger gene family whose roles have been better understood is the mammalian *Krox-20* gene, which functions in regulating hindbrain segmentation (5–7) and Schwann cell differentiation (8). Given the large number of $C_2$-$H_2$ Zn-finger genes that have been identified to date (4), it is surprising that *Krox-20* remains the only example that is segmentally expressed in rhombomeres of the hindbrain (9, 10). In this respect, characterization of developmental patterns of expression for newly discovered members of this gene family should help to identify other genes whose products may function in segmentation in higher organisms.

To gain insight into the possible role(s) of *PLZF*, we have now cloned its murine and avian homologues†† and studied their patterns of expression during embryogenesis. In both the mouse and chicken, *PLZF* displays a similar highly dynamic pattern of expression in the central nervous system (CNS). Within the hindbrain, an evolutionarily conserved pattern of expression correlates with the formation of rhombomeres and interrhombomeric boundaries, suggesting a fundamental role in hindbrain segmentation.

## MATERIALS AND METHODS

**cDNA Cloning and Whole-Mount *in Situ* Hybridization and Immunohistochemistry.** A random primed adult mouse heart λZapII (a gift from P. Chambon, Institut de Génétique et de Biologie Moléculaire et Cellulaire, Illkirch, France) and adult chicken heart λgt10 (Clontech) cDNA libraries were screened using $^{32}$P-labeled fragments of hPLZF cDNA, nt 1–1305 (3), and previously described conditions (11). The longest mouse and chicken cDNAs were sequenced and used as probes for *in situ* hybridization. Whole-mount *in situ* hybridization was done as described (12).

Mouse embryos were fixed in 4% (wt/vol) paraformaldehyde in phosphate-buffered saline for 30 min and subjected to whole-mount immunohistochemistry with the anti-PLZF polyclonal antiserum at 1:100 dilution essentially as described (13), except that TX-100 was used at 0.2%. The hindbrains of the stained embryos were flat-mounted as described (14). The

The publication costs of this article were defrayed in part by page charge payment. This article must therefore be hereby marked "*advertisement*" in accordance with 18 U.S.C. §1734 solely to indicate this fact.

Abbreviations: CNS, central nervous system; PLZF, promyelocytic leukemia zinc finger; dpc, days postcoitum; RT-PCR, reverse transcription/PCR; h*PLZF*, m*PLZF*, and c*PLZF*, human *PLZF*, murine *PLZF*, and chicken *PLZF*, respectively; r*x*, rhombomere *x*; HH, Hamburger and Hamilton.

**To whom reprint requests should be addressed.

††The sequences reported in this paper have been deposited in the GenBank data base [accession nos. Z47205 (m*PLZF*) and Z47206 (c*PLZF*)].

polyclonal anti-PLZF antiserum was raised against purified glutathione-*S*-transferase–hPLZF fusion protein and specifically detected human and mouse PLZF (mPLZF) proteins in immunoblotting, immunoprecipitation, and immunofluorescence experiments (data not shown).

**Reverse Transcription (RT)-PCR Analysis.** Total RNAs were prepared as described (3). A control cRNA, lacking 180 bp of the wild-type mPLZF(B) sequences, was derived from the mPLZF(B)Δ plasmid (see Fig. 1*B*). When different amounts of this template were subjected to RT-PCR in a background of 2.5 μg of mPLZF-negative total RNA, increased amounts of products were obtained (see Fig. 2*A*, lanes 1–4), indicating the semiquantitative nature of the method. All cDNAs were synthesized as before (3), using 2.5 μg of a given RNA and 1 pg of the mPLZF(B)Δ control cRNA. PCR amplifications were as described (3), except that one round of 25 cycles was done by using an annealing step at 54°C for 1 min and denaturation and extension for 25 sec at 95°C and 3 min at 72°C, respectively.

## RESULTS

**Cloning and Analysis of mPLZF cDNA.** The cDNA encoding mPLZF(B) protein was cloned by screening a mouse heart cDNA library. Four positive clones were isolated, and the longest clone (2.5 kb) was chosen for further analysis. Like its human counterpart (3), the mPLZF(B) cDNA possesses a 2019-bp-long open reading frame encoding a protein of 673 amino acids and $M_r$ 74,245 (Fig. 1*A*). Alignment of the deduced mouse and human PLZF(B) sequences revealed 96% amino acid identity, suggesting a high degree of functional conservation. The C-terminal region contains nine Zn-fingers, which constitute its DNA-binding domain (Fig. 1*B*). The N-terminal region contains a 100-amino acid domain that is highly conserved in a number of $C_2$-$H_2$ Zn-finger proteins. Recently, Bardwell and Treisman (15) have shown that in a protein called ZID this domain, termed POZ, can facilitate protein–protein interactions. However, the PLZF protein does not appear to interact *in vitro* with ZID (V. J. Bardwell, personal communication). An important functional role for the PLZF POZ domain is suggested by its remarkable evolutionary sequence conservation. Indeed, the POZ domain corresponds to the most highly conserved region between the described avian and mammalian PLZF sequences (see Fig. 1*A* and below). The conservation of the methionine codon (137) lying in both mammalian and avian mRNAs within conserved Kozak (16) sequences suggests that different N-terminal PLZF(A) and/or PLZF(B) proteins could be expressed with the shorter proteins lacking the POZ domain and potentially having distinct functional properties.

**Perinatal Induction of m*PLZF* Expression.** Initial Northern blot analysis indicated that the m*PLZF* gene was expressed at low levels. Therefore, we have used a semiquantitative RT-PCR procedure to facilitate the analysis in adult and fetal tissues. Although m*PLZF* expression was seen in a large number of tissues including the heart, lung, kidney, brain, liver, and spleen (Fig. 2 and data not shown), its perinatal upregulation was only observed in the kidney, liver, and heart (Fig. 2*A*). Interestingly, in all samples examined, only mRNAs encoding the B isoform of the mPLZF protein were detected.

To investigate the perinatal increase of m*PLZF* expression, we examined the temporal levels of its mRNAs in the livers and kidneys of mice homozygous for the $c^{3H}$ or $c^{14Cos}$ albino deletion (17). These mice fail to express normal levels of several essential liver enzymes, become hypoglycemic, and die shortly after birth. It has been shown that this phenotype is due to the absence of an enzyme (fumarylacetoacetate hydrolase) that functions in the last step of tyrosine metabolism (18). This metabolic defect is associated with profound effects on the levels of expression of many, but not all, structural and regulatory liver genes (17). Among the genes affected are those that encode the key transcription factors HNF-1, -4, and CEB/P-α, which regulate liver-specific gene expression (19). It is interesting that, as for the above factors, m*PLZF* expression is markedly decreased at birth, as compared with that in the wild-type animals (Fig. 2*B*). These results suggest that in the

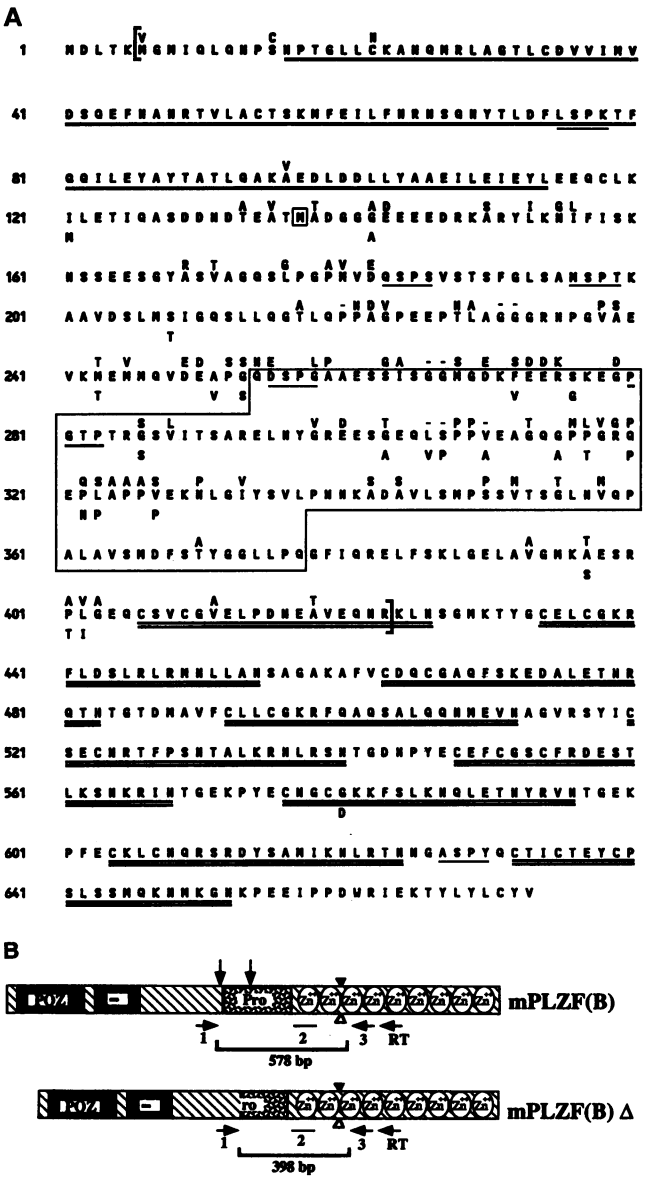


FIG. 1. (*A*) Deduced amino acid sequence of the mPLZF(B) protein and its conservation. The murine sequence is numbered on the left. The residues that differ from the mouse PLZF(B) sequences are indicated below (human) and above (chicken) their murine counterparts. Dashes indicate an absence of the corresponding amino acids. Brackets indicate the extent of the amino acid sequence derived from cPLZF(B) cDNA clone. Sequences that are encoded in the putative alternatively spliced exon are boxed. The POZ domain and Zn-finger sequences are underlined with heavy single and double lines, respectively. Conserved sequences of the potential proline-dependent phosphorylation sites are underlined with thin lines. The conserved methionine at position 137 is boxed. (*B*) Schematic diagrams of the mPLZF(B) and (B)Δ cDNAs, as well as strategy for RT-PCR analysis. Various structural regions are as indicated, and primers used for the RT-PCR (1 and 3) and hybridization (2) are shown below each diagram. Arrowheads between Zn-fingers 2 and 3 indicate position of a conserved exon/exon junction. Expected size of the amplification products is as indicated. Vertical arrows above the mPLZF(B) diagram indicate approximate positions of the two *Msc* I restriction enzyme sites used to create the mPLZF(B)Δ cDNA.

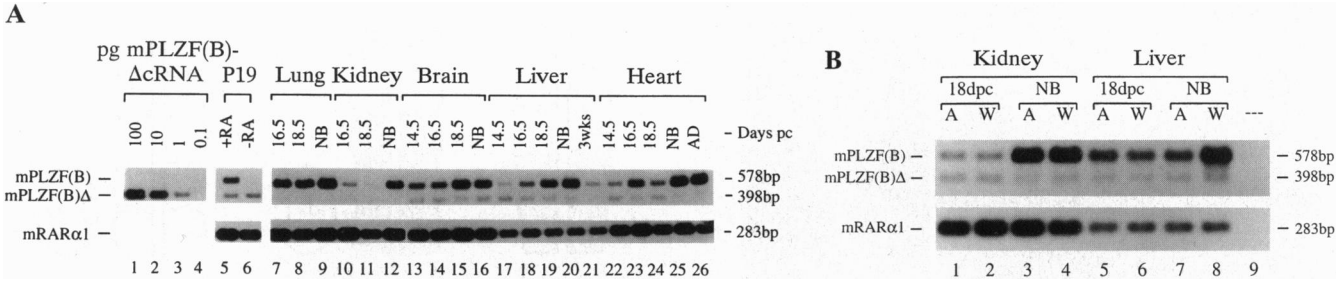


FIG. 2. (*A*) RT-PCR analysis of m*PLZF* expression in retinoic acid (RA)-treated and -untreated P19 cells, as well as fetal and newborn (NB) lung, kidney, brain, liver, and heart. Developmental stages and tissues are noted above each lane. Results obtained with RNAs derived from 3-week-old liver and adult (AD) heart are shown in lanes 21 and 26 for comparison. The lower blots show the results of control amplification of mRARα sequences from the corresponding samples. Lanes 1–4 show the results of amplification of decreased amounts of the mPLZF(B)Δ control cRNA, as indicated. The lengths of amplified cDNAs are indicated in bp on the right. (*B*) Comparison of m*PLZF* expression levels in kidneys (lanes 1–4) and livers (lanes 5–8) of 18 days postcoitum (dpc) and newborn wild-type animals (W) or animals with homozygous albino (A) deletion. Lane 9 corresponds to negative control where RNA was omitted from the reaction. All other markings are as described for *A*.

liver m*PLZF* may be a component of the same regulatory circuit as *CEB/P-α* and *HNF-1* and *-4*. Furthermore, because the albino deletions affect only gene expression in hepatocytes and proximal convoluted tubules of the kidney (20), the lack of induction of the m*PLZF* gene expression at birth in the mutant mice must reflect the changes in its expression that are occurring in the hepatocyte and not in the hemopoietic component of the liver. Nevertheless, levels of the m*PLZF* gene expression at 18 days postcoitum (dpc) appeared equal in both albino and the wild-type animals, suggesting that the earlier increase in its expression in the liver may indeed reflect the shift of hemopoiesis to this organ (21).

**Expression of m*PLZF* in the CNS During Embryogenesis.** When exposed to retinoic acid, P19 cells undergo neuronal differentiation (22). Induction of m*PLZF* expression during this time (Fig. 2*A*, lane 5) and its relationship to the hindbrain segmentation gene *Krox-20*, suggested the possibility that its product may play a role in CNS development. These findings prompted us to determine the patterns of m*PLZF* expression in the embryo during neurogenesis, with a particular focus on hindbrain segmentation.

In early neural plate-stage embryos (7.25 dpc), mPLZF can be detected in the neuroepithelia of the developing head folds (Fig. 3*A*), suggesting that expression of this gene may be an early marker of neuronal fate. Subsequently, at 7.5–8.0 dpc, high levels of mPLZF mRNAs are detected in the anterior edges of the head folds, the rostral extremity of the neural tube formation, and in the region of caudal neuropore (Fig. 3*B*). From 8.5 dpc we begin to see regional variations in CNS expression levels. There is strong staining in restricted domains of the hindbrain, midbrain, and parts of the forebrain, including the developing optic pit (Fig. 3 *C* and *D*), and lower levels of expression are seen over remaining regions of the forebrain, midbrain, and hindbrain throughout later stages (Fig. 3 *C–F*). Additionally, expression could be detected in the branchial arches, limb buds, otic vesicle, frontonasal mesenchyme, and mesonephros, but not in the heart, somites, or the notochord (Fig. 3 *E* and *F* and data not shown).

The specific spatiotemporal pattern of expression of the mPLZF mRNAs was closely paralleled by expression of mPLZF proteins (Fig. 3 *G* and *H*). The mPLZF protein is detected in the CNS, optic and otic vesicles, branchial arches, limb buds, and frontonasal mesenchyme. The granular appearance of the antibody staining, particularly prominent in the caudal neuropore region (Fig. 3*H*), is most likely due to the nuclear localization of the mPLZF proteins. As with mRNA, mPLZF proteins were essentially not expressed in the heart and the somites at these stages.

At 9.0 dpc, for both RNA and protein, strong staining could be observed in the first arch (Fig. 3*E*), and subsequently by 10.5 dpc, such staining could be detected in both the second and third branchial arches (Fig. 3 *F–H*). This pattern reflects the temporal order in the production of rhombencephalic neural crest and its migration into the branchial arches (Fig. 4*A*). With time, expression in cranial neural crest is down-regulated and appears only in a subset of cells. There is expression in the surface ectoderm, branchial clefts, and underlying superficial mesenchyme, as seen by the higher staining density around the edge of each arch (Fig. 3 *E–H*).

**Expression During Hindbrain Segmentation.** From 8.5 to 10.5 dpc the hindbrain becomes morphologically subdivided into lineage-restricted units termed rhombomeres (23), whose formation is tightly linked with segmental expression of several developmental regulatory genes such as *Krox-20, Sek-1*, and *Hox* genes (24). It is precisely during this period that m*PLZF*

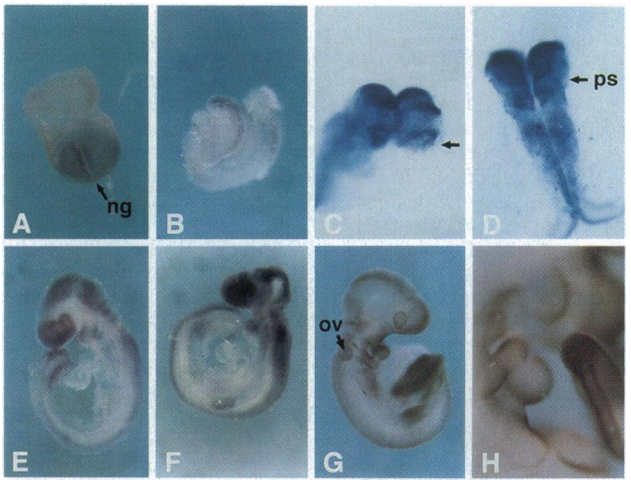


FIG. 3. Whole-mount *in situ* hybridization and immunohistochemistry of mouse embryos with an antisense mPLZF(B) cRNA and anti-PLZF antibodies. (*A*) Presomitic stage embryo (7.25 dpc) showing mPLZF expression in the developing head folds. (*B*) Lateral view of 8.0-dpc embryo, five to seven somites. (*C* and *D*) Different views of cephalic neuroepithelium of ≈8.5-dpc-old embryo demonstrating down-regulation of m*PLZF* expression in discrete regions of the prospective forebrain and hindbrain. Arrow in *C* points toward the optic pit. (*E*) Lateral view of a 9.0-dpc embryo showing mPLZF mRNA expression in the CNS, branchial arches, and frontonasal mesenchyme. (*F*) Lateral view of a 10.5-dpc embryo. mRNA expression in the limb buds, mesonephros, and the otic vesicle is also apparent at this later stage. Note specific regional down-regulation of mPLZF mRNA levels in the forebrain and hindbrain. (*G*) Lateral view of 9.5-dpc embryo revealing pattern of antibody staining in the CNS, frontonasal mesenchyme, branchial arches, and forelimb bud. (*H*) Magnification of the posterior neuropore region of a similar embryo as in *G*. ng, Neural groove; ov, otic vesicle; r, rhombomere; ps, preotic sulcus.

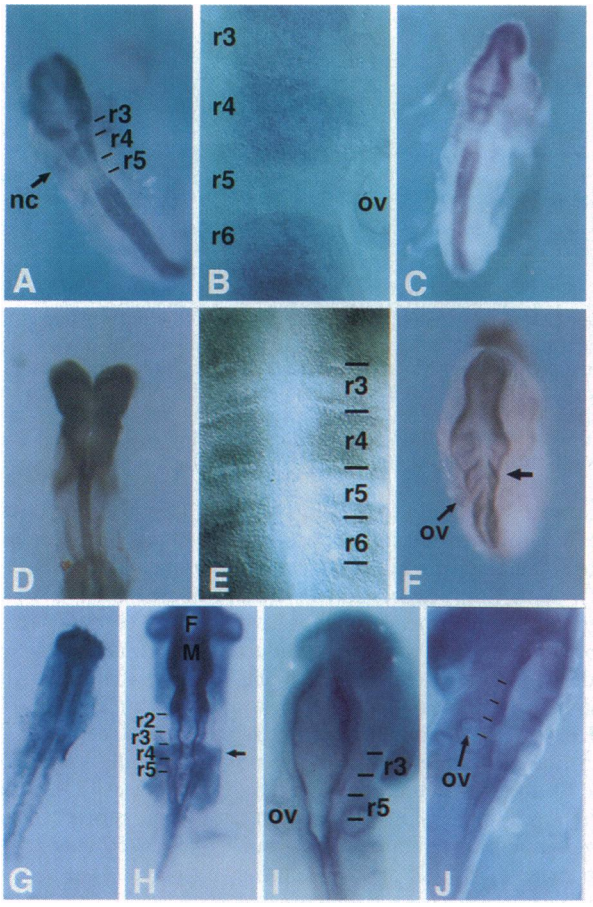


FIG. 4. Conserved segmental patterns of m*PLZF* expression during hindbrain development. (*A*) A 9.0- to 9.5-day-old embryo showing down-regulation of m*PLZF* expression in the regions encompassing rhombomere 3 (r3) and r5. Expression in r4 neural crest (arrow) is also visible. (*B*) Flat-mount of the stained hindbrain region containing r3 and r5 of an embryo at a similar developmental stage as in *A*. Note down-regulation of m*PLZF* expression in central parts of r3 and r5. (*C*) Expression at 10.0 dpc demonstrating increased m*PLZF* expression at rhombomeric boundaries. (*D*) An 8.0-dpc-old embryo showing expression of mPLZF protein(s) in the developing CNS. (*E*) Flat-mount of 9.75-dpc embryo showing mPLZF protein expression in the hindbrain. Note lack of staining in the floor plate. (*F*) Dorsal view of 10.0-dpc-old embryo showing striped expression of the mPLZF protein around rhombomeric boundaries. Arrow points to r3/r4 boundary. (*G*) Whole-mount *in situ* hybridization of HH stage 10 chicken embryo showing high levels of c*PLZF* expression in cephalic neuroepithelium. (*H*) At Hamburger and Hamilton (HH) stage 11, down-regulation of expression in r2, r3, and, to a lesser degree, in r5 becomes apparent. Arrow points to PLZF mRNA-positive neural crest streaming from r4. (*I*) Stages HH14 revealing more complete down-regulation of c*PLZF* expression in r5. (*J*) Stage HH15 showing that c*PLZF* expression is being up-regulated at rhombomeric boundaries. F, forebrain vesicle; M, midbrain vesicle; ov, otic vesicle; nc, neural crest. Dashes indicate approximate positions of rhombomeric boundaries.

displays a highly dynamic pattern of expression in the rhombencephalon and, therefore, we have examined whether this pattern of expression can be correlated with the process of segmentation. Fig. 4*A* shows down-regulation of m*PLZF* expression in r3 and r5 of a 9.0- to 9.5-dpc embryo. Detailed analysis at higher resolution (Fig. 4*B*) shows that at this stage down-regulation occurs only in the central portion of r3 and r5. Therefore, expression apparently persists in r3 and r5 in cells lying adjacent to the rhombomeric boundaries. At 10.0 dpc, down-regulation of mPLZF expression also becomes apparent in the even-numbered rhombomeres, and strong staining at the boundaries can be observed in all the rhombomeres (Fig. 4*C*).

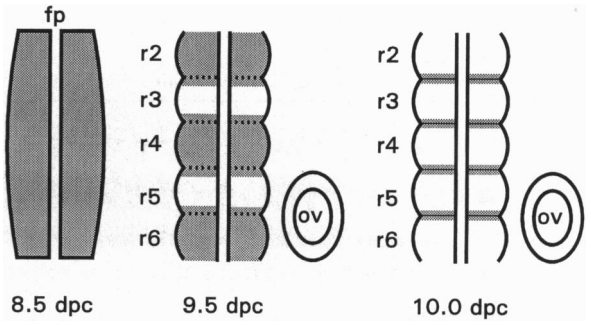


FIG. 5. Summary of segmental expression of *PLZF* in the mouse hindbrain. At 8.5 dpc, expression is uniform in the neural tube, and by 9.5 dpc, expression in the center of r3 and r5 has been down-regulated. By 10.0 dpc, expression in all rhombomeres has been down-regulated, leaving expression only at rhombomere boundaries; this same sequence of events is observed in the chicken, except down-regulation occurs in the center of r2 and r3 at the same time. ov, Otic vesicle; fp, floor plate; r, rhombomere.

High levels of expression remain in other anterior and posterior regions of the neural tube. In a flat-mount of the hindbrain at 9.5–10.0 dpc, rhombomeric boundaries are clearly apparent, and anti-PLZF antibodies reveal higher levels of protein expression over several cell diameters on either side of the boundaries (Fig. 4*E*). As a consequence of the elevated expression over the rhombomeric boundaries, the entire hindbrain regions adopt a characteristic striped appearance (Fig. 4 *C* and *F*). Throughout all of these stages expression in the floor plate was not detected. Fig. 5 graphically summarizes the progressive pattern of mPLZF mRNA and protein expression during hindbrain development.

**Cloning of Chicken *PLZF* (c*PLZF*) and Its Expression in the Developing Hindbrain.** The process of hindbrain segmentation has been conserved throughout vertebrate evolution (10) and is well characterized in the chicken (13). Therefore, to determine whether the segmental patterns of *PLZF* expression were also conserved, we have cloned the cPLZF cDNA. Sequencing analysis revealed an open reading frame encoding a protein with high homology to amino acids 6–423 of the mouse and human homologues (indicated with brackets in Fig. 1*A*). The overall sequence identity between the mPLZF and cPLZF sequences is ≈80%.

Initial results clearly demonstrate c*PLZF* expression in the early neuroepithelium (highly elevated in the cephalic region) and modulation of its expression in a rhombomere-specific manner (Fig. 4 *G–J*). At stage HH10 of chicken development (25), c*PLZF* expression appeared high in the cephalic neural folds and decreased within the prospective hindbrain region, remaining at lower levels throughout the posterior CNS (Fig. 4*G*). At stage HH11, high levels of c*PLZF* expression were detected in the forebrain, optic pits, midbrain, and the anterior region of the hindbrain corresponding to prospective r1. The expression abruptly decreased in r2 and r3, increased moderately in r4, and was lower again in r5 (Fig. 4*H*). By stage HH14, the decrease in r5 was completed (Fig. 4 *H* and *I*) and, by HH15, we begin to see higher levels of c*PLZF* expression at rhombomeric boundaries (Fig. 4*J*). As in the mouse embryo, there also was expression in the branchial arches and optic pits, as well as in the r4 neural crest (Fig. 4*H*, arrow) and essentially no expression in the developing heart and somites. These evolutionarily conserved patterns of expression suggest that PLZF could play a common functional role in vertebrate hindbrain segmentation.

## DISCUSSION

Spatiotemporal patterns of m*PLZF* expression suggest that its products may function during the development of a number of

organ systems and in different cell types. Here we have particularly focused on the developing CNS. The dynamic changes in *PLZF* expression, leading to high levels at rhombomeric boundaries, occur precisely when expression of other molecular markers of segmentation, such as *Krox-20, Sek-1*, and *Hox* genes (10, 24), becomes restricted in the hindbrain. The down-regulation of *PLZF* expression in r3 and r5 at 9.0 dpc follows up-regulation of *Krox-20* and *Sek-1* in these rhombomeres, suggesting that *PLZF* could be a target of their activities.

Initially, rather uniform expression of the *PLZF* gene, which later subdivides into the more segmented pattern, is reminiscent of the spatiotemporal pattern of expression of the *Drosophila* pair-rule segmentation gene odd-paired (26). Interestingly, the highest levels of odd-paired expression also occur at boundaries separating adjacent metameric units (parasegments), which possess distinct morphogenic and histogenic properties during fly development. In the avian embryo, boundaries between rhombomeres have indeed been shown to represent a lineage restriction, preventing mixing of cells with distinct developmental potentials (23). The pattern of elevated gene expression in cells surrounding rhombomeric boundaries has not been previously observed for any other vertebrate transcription factor and suggests that PLZF activity is involved at a specific stage in establishment and/or maintenance of a boundary cell phenotype.

Although morphologically and physiologically less clear, organization of the forebrain into metameric units called prosomers or neuromers during vertebrate development is also believed to occur (27, 28). In analogy with the hindbrain, many genes, often encoding transcription factors, have been shown to possess expression domains coincident with the proposed neuromeric boundaries of the forebrain, thus supporting the neuromeric model for its organization during development. It is worth noting that at 10.5 dpc, in addition to the hindbrain, expression of the *PLZF* gene displays some regionalization in the more anterior areas of the developing brain. mPLZF mRNAs appear higher in specific telencephalic regions than in the diencephalon and mesencephalon (Fig. 3*F*). Furthermore, there appears to be a sharp decrease in its levels of expression in the diencephalon (possibly at the boundary between prosomeres 1 and 2, which mark the border between the protectum and dorsal thalamus) and at the mid/hindbrain isthmus (27). Given its expression in the hindbrain, which is linked with the developing rhombomeres, *PLZF* may also prove to be an important gene among those whose expression patterns give credence to the neuromeric model of forebrain organization. In conclusion, the evolutionary conservation of its segmented expression in the hindbrain, particularly at the rhombomeric boundaries, strongly suggests that *PLZF* is likely to play an important role within the cascade of regulatory genes that control segmentation processes leading to hindbrain regionalization, and perhaps also the forebrain, during development.

We thank L. Wiedemann, T. Enver, M. Greaves, and other members of the Institute for helpful comments and P. Chambon for providing the mouse heart cDNA library. N.B. thanks Dr. P. Barton, Prof. M. Yacoub, and the British Heart Foundation for their support. This research was supported by The Leukaemia Research Fund of Great Britain, National Institutes of Health Grant CA59936-01, and the Medical Research Council. A.G. is a Beit Memorial Research Fellow.

1. Warrell, R. P., de The, H., Wang, Z.-Y. & Degos, L. (1993) *N. Engl. J. Med.* **329,** 177–189.
2. Zelent, A. (1994) *Br. J. Haematol.* **86,** 451–460.
3. Chen, Z., Brand, N. J., Chen, A., Chen, S.-J., Tong, J.-H., Wang, Z.-Y., Waxman, S. & Zelent, A. (1993) *EMBO J.* **12,** 1161–1167.
4. El-Baradi, T. & Pieler, T. (1991) *Mech. Dev.* **35,** 155–169.
5. Schneider-Maunoury, S., Topilko, P., Seitanidou, T., Levi, G., Cohen-Tannoudji, M., Pournin, S., Babinet, C. & Charnay, P. (1993) *Cell* **75,** 1199–1214.
6. Swiatek, P. J. & Gridley, T. (1993) *Genes Dev.* **7,** 2071–2084.
7. Sham, M. H., Vesque, C., Nonchev, S., Marshall, H., Frain, M., Das Gupta, R., Whiting, J., Wilkinson, D., Charnay, P. & Krumlauf, R. (1993) *Cell* **72,** 183–196.
8. Topilko, P., Schneider-Maunoury, S., Levi, G., Baron-Van Evercooren, A., Ben Younes Chennoufi, A., Seitanidou, T., Babinet, C. & Charnay, P. (1994) *Nature (London)* **371,** 796–799.
9. Lumsden, A. (1990) *Trends NeuroSci.* **13,** 329–335.
10. Krumlauf, R. (1994) *Cell* **78,** 191–201.
11. Zelent, A., Krust, A., Petkovich, M., Kastner, P. & Chambon, P. (1989) *Nature (London)* **339,** 714–717.
12. Wilkinson, D. G. (1992) in *In Situ Hybridization: A Practical Approach*, ed. Wilkinson, D. G. (IRL, Oxford), pp. 75–83.
13. Lumsden, A. & Keynes, R. (1989) *Nature (London)* **337,** 424–428.
14. Marshall, H., Nonchev, S., Sham, M. H., Muchamore, I., Lumsden, A. & Krumlauf, R. (1992) *Nature (London)* **360,** 737–791.
15. Bardwell, V. J. & Treisman, R. (1994) *Genes Dev.* **8,** 1664–1677.
16. Kozak, M. (1986) *Cell* **44,** 283–292.
17. Gluecksohn-Waelsch, S. & DeFranco, D. (1991) *BioEssays* **13,** 557–561.
18. Kelsey, G., Ruppert, S., Beermann, F., Grund, C., Tanguay, R. M. & Schütz, G. (1993) *Genes Dev.* **7,** 2285–2297.
19. Tonjes, R. R., Xanthopoulos, K. G., Darnell, J. E., Jr., & Paul, D. (1992) *EMBO J.* **11,** 127–133.
20. Ruppert, S., Kelsey, G., Schedl, A., Schmid, E., Thies, E. & Schütz, G. (1992) *Genes Dev.* **6,** 1430–1443.
21. Medvinsky, A. L. (1993) *Dev. Biol.* **4,** 333–340.
22. Jones-Villeneuve, E. M. V., McBurney, M. W., Rogers, K. A. & Kalnins, V. I. (1982) *J. Cell Biol.* **94,** 253–262.
23. Fraser, S., Keynes, R. & Lumsden, A. (1990) *Nature (London)* **344,** 431–435.
24. Wilkinson, D. G. (1993) *BioEssays* **15,** 499–505.
25. Hamburger, V. & Hamilton, H. (1951) *J. Morphol.* **88,** 49–92.
26. Benedyk, M. J., Mullen, J. R. & DiNardo, S. (1994) *Genes Dev.* **8,** 105–117.
27. Puelles, L. & Rubenstein, J. L. R. (1993) *Trends NeuroSci.* **16,** 472–479.
28. Figdor, M. C. & Stern, C. D. (1993) *Nature (London)* **363,** 630–634.